Journal of Power Sources 196 (2011) 7347–7354

Contents lists available at ScienceDirect

Journal of Power Sources

journal homepage: www.elsevier.com/locate/jpowsour

A techno-economic comparison of fuel processors utilizing diesel for solid oxide fuel cell auxiliary power units

Pedro Nehter[a,*], John Bøgild Hansen[b], Peter Koch Larsen[a]

[a] TOPSOE FUEL CELL, Nymøllevej 66, DK-2800 Lyngby, Denmark
[b] Haldor Topsoe A/S, Nymoellevej 55, DK-2800 Lyngby, Denmark

ARTICLE INFO

Article history:
Received 23 June 2010
Received in revised form 24 August 2010
Accepted 6 September 2010
Available online 29 September 2010

Keywords:
Diesel
Partial oxidation
Autothermal
SOFC
APU
Economic

ABSTRACT

Ultra-low sulphur diesel (ULSD) is the preferred fuel for mobile auxiliary power units (APU). The commercial available technologies in the kW-range are combustion engine based gensets, achieving system efficiencies about 20%. Solid oxide fuel cells (SOFC) promise improvements with respect to efficiency and emission, particularly for the low power range. Fuel processing methods i.e., catalytic partial oxidation, autothermal reforming and steam reforming have been demonstrated to operate on diesel with various sulphur contents. The choice of fuel processing method strongly affects the SOFC's system efficiency and power density.

This paper investigates the impact of fuel processing methods on the economical potential in SOFC APUs, taking variable and capital cost into account. Autonomous concepts without any external water supply are compared with anode recycle configurations. The cost of electricity is very sensitive on the choice of the O/C ratio and the temperature conditions of the fuel processor. A sensitivity analysis is applied to identify the most cost effective concept for different economic boundary conditions.

The favourite concepts are discussed with respect to technical challenges and requirements operating in the presence of sulphur.

1. Introduction

There are 3,573,000 Class 8 Heavy Duty trucks in the United States and 526,000 in Canada [1]. A certain percentage of these vehicles are used for long-haul driving, which are left idling overnight, to ensure that heat and power is available to the driver. The power is needed for lighting, heating, air-conditioning, and comfort-items such as microwave ovens and coffeemakers.

The U.S. Environmental Protection Agency (EPA) estimates that idling trucks in USA annually consume >3.8 billion litres of fuel producing emissions of 11 million tons of CO_2, 180,000 tons of NOX and 5000 tons of particulate matter [2]. Moreover, many US states have legislation pending that limits idling in some form to prevent air pollution and reduce noise emissions.

An efficient, low-noise solid oxide fuel cell (SOFC) based APU can provide a way to reduce air pollution and noise emissions. SOFC promise improvements towards efficiency and emission, particularly for the low power range.

Standard, Ultra-low sulphur diesel (ULSD) is the preferred fuel for mobile auxiliary power unit (APU) applications. Such fuels have an average sulphur content of 6 ppm, although the spec limit is 15 ppm [3]. The commercial available technologies in the kW-range are combustion engine based gensets, achieving system efficiencies about 20%.

The requirements for a truck APU are difficult to quantify, as different end-users give different answers. However, a general picture is that the following requirements must be met:

- 20,000 h lifetime.
- 50–100 thermal cycles per year.
- <65 dB(A) noise level.
- Fit into existing infrastructure: servicing with main engine, integration on truck frame, etc.

If one can make a fuel cell-based APU meeting these criteria with a positive return on investment, a strong market demand will make it a successful product. The baseline cost for truck idling is given in Table 1.

* Corresponding author. Tel.: +45 4527 8482; fax: +45 4527 8482.
E-mail address: nehter@aol.com (P. Nehter).

0378-7753/$ – see front matter.
doi:10.1016/j.jpowsour.2010.09.011

Table 1
Cost for truck idling [4].

	Truck idling
Electrical net efficiency	4%
Power average [kWel]	1.3
Power peak [kWel]	3.9
Electrical work [kWh year^{-1}] (1830 h year^{-1})	2379
Fuel consumption [gal year^{-1}] (37 kWh gal^{-1})	1607
Fuel cost [$ year^{-1}] (2.9$ gal^{-1})	4661
Maintenance cost [$ h^{-1}]	0.16
Maintenance cost [$ year^{-1}]	292
Variable cost (fuel + maintenance) [$ year^{-1}]	4953

2. Diesel fuel processor

2.1. Intrinsic exergetic efficiency of fuel processors

The nature of the fuel and the catalyst determine the challenges a fuel processor will face. Nickel containing SOFC anodes have a high activity towards the electrochemical oxidation of hydrogen but are very prone to carbon formation from higher hydrocarbons. Higher hydrocarbon containing fuels should be converted to a mixture of hydrogen, water, carbon monoxide, carbon dioxide and methane in order to avoid carbon formation on the anode. The most established processes for this conversion step are the steam reforming (SR), partial oxidation (CPO/POX) and autothermal reforming (ATR). The autothermal reforming is a combination of steam reforming and partial oxidation. The mechanism of the reaction is the occurrence of partial oxidation in the initial part of the bed producing steam and heat to drive steam reforming in the downstream part. Steam reforming is a principle technology to generate hydrogen using nickel catalyst and natural gas feedstock, where a hydrocarbon reacts with steam to form carbon monoxide and hydrogen. The key feature of steam reforming is the fact that it is a strongly endothermic reaction. A rather small amount of heat is released by a simultaneously occurring shift reaction which forms hydrogen and carbon dioxide from carbon monoxide and water The reformate contains a few ppm methane at high reforming temperatures >750 °C and up to 15% methane for reforming temperatures <550 °C. The methanation of CO can in fact make the overall steam reforming of higher hydrocarbons exothermic at low temperatures. Simulated equilibrium compositions, using $C_{14}H_{30}$ n-tetradecane to represent the diesel, are given in Fig. 1.

The endothermic nature of the steam reforming on the SOFC anode makes methane in the reformate an effective cooling agent which reduces parasitic losses for cathode air compression. The SOFC's heat is upgraded to chemical energy internally by supplying the reforming reaction entropy with reaction entropy from the hydrogen oxidation in a regenerative way.

$$C_\alpha H_\beta + \alpha H_2O \leftrightarrow \left(\frac{\beta}{2} + \alpha\right) H_2 + \alpha CO \quad \text{Steam reforming (endothermic)} \tag{1}$$

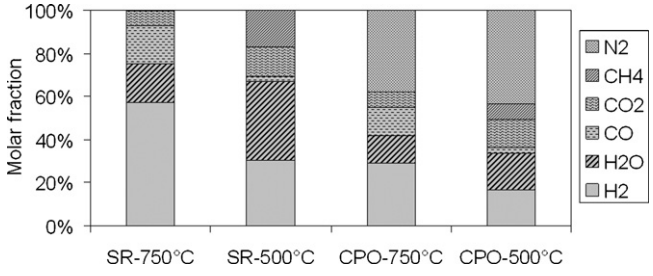

Fig. 1. Simulated equilibrium compositions for $C_{14}H_{30}$ n-tetradecane as diesel replacement; O/C = 2.

$$CO + H_2O \leftrightarrow H_2 + CO_2 \quad \text{Shift reaction (exothermic)} \tag{2}$$

Partial oxidation (Eq. (3)) is the oxidation of the hydrocarbon with a sub-stoichiometric amount of oxygen which is typically supplied by air in the presence of catalyst (CPO) or without a catalyst (POX). The POX typically requires a higher oxygen to carbon ratio than the CPO in order to achieve appropriate temperatures to avoid carbon formation. The reformate of a CPO or POX contain below <1% methane. Higher methane contents (<10%) can be achieved by coupling the CPO with an exothermic methanation [5] in order to equilibrate the reformate at a temperature <600 °C. The exothermic heat duty of methanation is used downstream in the SOFC in the reverse way to cool the stack by endothermic steam reforming.

$$C_\alpha H_\beta + \left(\frac{\alpha}{2}\right) O_2 \rightarrow \frac{\beta}{2} H_2 + \alpha CO \quad \text{Partial oxidation (exothermic)} \tag{3}$$

Comparing the reformate compositions (Fig. 1) at 500 °C and 750 °C show the same tendency for the SR and CPO. Increasing the reactor temperature from 500 °C to 750 °C affects the equilibrium composition as follows:

- The hydrogen/water ratio and carbon monoxide/carbon dioxide ratio increases.
- The shift equilibrium lead to a higher carbon monoxide content in the reformate.
- The methane content is below 1%.

For the SOFC, hydrogen content is not as important as it is for a proton conducting low temperature fuel cells as it is generated both from methane via steam reforming and CO via water gas shift on the anode. The utilisation of carbon monoxide occurs indirectly at the anode via the shift reaction. The Nernst potential for the oxidation of hydrogen and carbon monoxide remains the same as long as the shift reaction is in its equilibrium [6].

The performance of a fuel processor and its impact on the system performance can be evaluated by exergetic analyses. Based on the second law of thermodynamics, exergy is defined as maximum work that can be obtained from a given form of energy by equilibrating it with the environmental conditions. An exergy stream covers all kinds of potential work like chemical, electrical, thermal and mechanical. For a fuel containing process stream the exergy is equal to the Gibbs free energy calculated for environmental conditions as a reference state. The environment is defined as T_{amb} = 298.15 K, p_{amb} = 1 bar, , $x_{O_2} = 0.202$, $x_{Ar} = 0.00906$, $x_{H_2O} = 0.03171$, $x_{CO_2} = 0.00031$.

$$E = \Delta G_{amb} = \Delta H_{amb} - T_{amb}\Delta S_{amb} = (H - H_{amb}) - T_{amb}(S - S_{amb}) \tag{4}$$

The exergy loss of each process is the difference between the exergy output and input stream.

$$E_{loss} = E_{in} - E_{out} \tag{5}$$

The exergetic efficiency is defined as ratio of the output and input exergy. The input exergy for a power generating process is typically fuel's exergy which is for many fuels almost equal to the LHV.

$$\eta_{ex} = \frac{E_{out}}{E_{in}} \tag{6}$$

The separation of the exergy of a process stream and the exergy loss of specific components into the different types of potential

work provides a transparent picture of the way exergy losses affect the system efficiency. A loss in chemical exergy has a strong impact on the electrical efficiency of a fuel cell system. If fuel is partially oxidised before it enters the fuel cell, the chemical exergy strongly decrease even if the dissipated exergy of this pre-combustion process is partly captured by the exergy of heat generated by the partial oxidation. The partial oxidation results in lower electrical system efficiency even if the exergetic efficiency for the pre-combustion is high. This can be misleading because the partial oxidation can be one of the major losses of chemical exergy. An intrinsic exergetic efficiency of the fuel processor is defined by taking only the chemical exergy at the temperature and pressure conditions of the SOFC into account.

$$\eta_{\mathrm{ex,int\,FP}} = \frac{W_{\mathrm{rev,SOFC}}}{E_{\mathrm{fuel}}} \tag{7}$$

The exergy of reaction heat of the reversible SOFC does not directly contribute to the work of the SOFC and is thereby considered to be dissipated into the environment. The residual chemical exergy which could be extracted from the total exergy is thus identical to the maximum work which could be converted by a reversible SOFC. The intrinsic exergetic efficiency of the fuel processor turns thus into an upper exergetic efficiency for the entire SOFC system as long as it is a pure fuel cell system decoupled from any heat engines and operating at atmospheric conditions. The reversible work covers the chemical part of the exergy which could be converted by a reversible SOFC taking the change in fuel gas composition due to the fuel utilisation into account. The air composition at the cathode is chosen to be constant to decouple indirect effects of the fuel composition on the cooling demand of the cell and thus on the oxygen content. The average Nernst voltage is considered to be the driving force, which is a function of the reversible work of the hydrogen oxidation. The reversible work of the hydrogen oxidation can be determined by the free reaction enthalpy as follows:

$$W_{\mathrm{rev,SOFC}} = \int_{\mathrm{uf},1}^{\mathrm{uf},2} \Delta^r G_{(750^\circ\mathrm{C},p)}\,\mathrm{duf} \tag{8}$$

Fig. 2 illustrates the changes in LHV (full line) and reversible work (dashed line) which occur in an equilibrium steam reformer at 750 °C (left figure) and at 500 °C (right figure). The reformate composition is simulated as illustrated in Fig. 1. The LHV of reformate is calculated by the sum of LHV of hydrogen, carbon monoxide and methane.

At 750 °C the heat duty of the reforming is 2754 kJ and 634 kJ at 500 °C. The LHV of the reformate is thus much higher at a high reformer temperature (750 °C) which is due to the higher hydrogen and less methane content. The difference between the LHV of reformate and the reversible work is approximately equal to the reversible heat of reaction. The reversible heat has to be released from the SOFC even if the cell would operate under reversible conditions. For a reformer temperature of 500 °C the reversible heat of the reformate is much lower due to the higher methane content. The reversible work to LHV ratio of the reformate (Wrev/LHV; Table 2) indicates that the cooling demand of the SOFC will be significantly higher at 750 °C reforming temperature. The reformate's LHV contains 29% of reversible heat at 750 °C reforming temperature and 17% at 500 °C reforming temperature.

The intrinsic exergetic efficiency of the high and the low temperature reformer are almost equal with 87% at 750 °C and 86% at 500 °C. The commonly used thermal efficiency of a fuel processor which relates the LHV of the reformate to the LHV of the diesel would be misleading comparing the thermal efficiencies at 750 °C and 500 °C reforming temperature. The thermal efficiencies would be quite different for the two reforming temperatures even if the potential work content of the reformate is almost constant. The total exergetic efficiencies are 98% and 99% for the steam reformer. For the total exergetic efficiency it is important to keep in mind that the exergy of heat is also involved. The total exergetic efficiency represents the upper limit of reformate's potential work which could be extracted by a combined reversible fuel cell and heat engine.

Fig. 3 illustrates the penalty in reversible work using a non-adiabatic CPO as fuel processor. The low temperature case at 500 °C on the right-hand side of the figure involves a methanation post-process in order to equilibrate the gas at this temperature. Around 32% of the diesel is pre-combusted within the CPO for both cases at 750 °C and 500 °C equilibration temperature. An equivalent amount of electrons which could contribute to the work generated in the downstream SOFC is lost by the partial oxidation. The loss of reversible work is 41.5% for the 750 °C and 42% for the 500 °C case. The loss in reversible work is converted into heat which partly compensates the exergetic loss. Thus, the total exergetic efficiency (86–89%) is much higher than the intrinsic exergetic efficiency (58–58.5%). However, the low intrinsic exergetic efficiency of the CPO will reduce the electrical system efficiency significantly.

2.2. Operation conditions of diesel fuel processor

The intrinsic efficiency of the fuel processor and the thus the system efficiency is mainly affected by the O_2/C ratio, which can also by expressed by the excess air ratio λ for a given fuel $C_\alpha H_\beta$. The index α is the number of carbon and β the number of hydrogen atoms per hydrocarbon molecule $C_\alpha H_\beta$.

$$\lambda_{\mathrm{diesel}} = \frac{\alpha(\mathrm{O_2/C_{diesel}})}{\alpha + (\beta/4)} \tag{9}$$

The O_2/C ratio varies in a broad range for the different fuel processors. The catalytic activity of the fuel processor and the higher hydrocarbon content of the reformate is strongly coupled with numerous effects governed by the thermal conditions, mixing of the diesel with air or anode recycle gas, sulphur content, O/C and S/C ratios. Carbon deposition caused by higher hydrocarbons or Boudouard equilibrium has to be avoided in order to ensure long term stability of the SOFC's anode. Carbon deposition caused by the Boudouard reaction can be thermodynamically approximated by its equilibrium. The minimum O/C ratio

$$\frac{\mathrm{O}}{\mathrm{C}} = 2\frac{\mathrm{O_2}}{\mathrm{C}} + \frac{\mathrm{S}}{\mathrm{C}} \tag{10}$$

of the carbon free operation regime of $C_{14}H_{30}$ is in the range of 1.5–3 depending on the O_2/C ratio and the temperature. Most of the diesel fuel processors operate at an O/C ratio of 2–3. Higher O/C ratios than 3 cannot exclusively be supplied by an anode gas recycle. An additional external water supply would be one solution to achieve higher O/C ratios than 3 (Fig. 4).

Adiabatic steam reforming of diesel has been demonstrated over 1000 h at an O/C of around 2.5 [7]. Autothermal reformer is able to operate at O_2/C ratios around 0.47 [8] which is equivalent to an excess air ratio of 0.3 using $C_{14}H_{30}$ as diesel replacement. A typical operation range for CPOs (often called ATR if water is present) is an excess air ratio of 0.32–0.4 [9] which correspond with an O_2/C ratio of 0.5–0.61.

3. Impact of sulphur on cell performance

With respect to the impact of sulphur on the electrochemical performance of nickel based SOFC cells there is a consensus in the literature that:

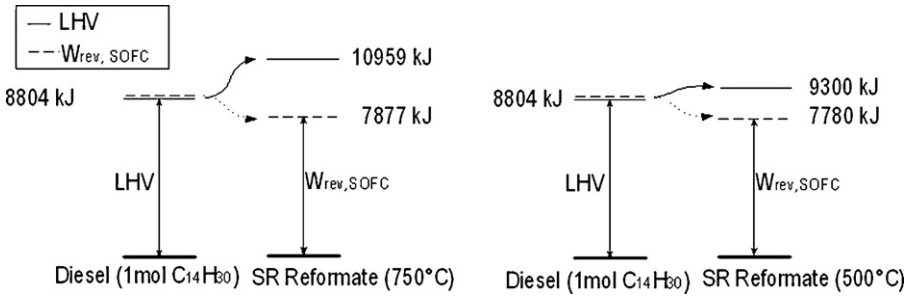

Fig. 2. Energy conversion of a steam reformer at equilibrium ($C_{14}H_{30}$).

Table 2
Steam reformer and catalytic partial oxidation equilibrium simulation.

	SR – 750 °C	SR – 500 °C	CPO – 750 °C	CPO – 500 °C
O_2/C	0	0	0.5	0.5
S/C	2	2	1	1
O/C	2	2	2	2
LHV reformate [kJ mol^{-1} $C_{14}H_{30}$]	10,959	9300	7488	6418
Qreforming [kJ mol^{-1} $C_{14}H_{30}$]	2754	634	−537	−2191
(Reformer inlet temperature = 400 °C)	Endothermic	Endothermic	Exothermic	Exothermic
Wrev $C_{14}H_{30}$ [kJ mol^{-1}]	9017	9017	9017	9017
Wrev reformate, SOFC 750 °C [kJ mol^{-1} $C_{14}H_{30}$]	7877	7780	5263	5223
Wrev_reformate/LHV_reformate	0.71	0.83	0.70	0.81
Intrinsic exergetic efficiency	87%	86%	58.5%	58%
Exergy reformate [kJ mol^{-1} $C_{14}H_{30}$]	11,157	9755	7935	6845
Exergetic efficiency	98%	99%	89%	86%

- The deactivation by H_2S increases by lowering temperature.
- The effect levels off as the H_2S concentration increases.
- The impact of sulphur is less at a high current density.

There is also general agreement that sulphur has an immediate impact on the electrochemical performance of Ni anodes [10].

The long term effects and the degree of recovery achievable after sulphur is removed from the feed stream again remain, however, still somewhat unclear as the reported data on long duration experiments in the literature is scarce, but exposure to a few ppm of hydrogen sulphide as suggested in this paper seem to be acceptable [11,12].

Extensive work on steam reforming catalyst has shown that the sulphur coverage on nickel can be very well described by a Temkin like isotherm:

$$\theta_s = 1.45 - 9.53 \times 10^{-5} T + 4.17 \times 10^{-5} T \ln\left(\frac{p_{H_2S}}{p_{H_2}}\right) \quad (11)$$

where θ_s is the fractionally coverage of sulphur of the nickel surface. This formula has also been demonstrated to describe the performance loss encountered in Ni-YSZ cells [13] (Fig. 5):

$$\mathrm{Pl} = k * (\theta s - \theta\ \mathrm{min}) = 53.8\theta s - 32.2 \quad (12)$$

with $R^2 = 0.985$.

The data cover hydrogen sulphide concentrations from 0.05 to 50 ppm and temperatures from 700 to 900 °C. Other data at 1000 °C as well as data from coal gasifier gases was also well described. The impact of sulphur would be different with other anode compositions, those based on SSZ e.g., and at different current densities, but for the sake of illustration the formula ion Eq. (12) has been used in the following.

It is also known from catalysis research that steam methane reforming activity depends on $(1 - \theta s)$ raised to the third power. Very low conversions of the small amounts of methane from the diesel reformer can thus be expected [14], and the effect has been included in our simulations. The impact of sulphur on the shift reaction has not yet been quantified [10,15–17], but is probably in between the impact on the steam reforming reaction and the hydrogen oxidation. As the shift reaction, however, is normally very fast with gas compositions considered in this paper the impact on the shift reaction has been ignored in our calculations.

4. System configurations

For the comparison of the fuel processors, two different process configurations have been chosen. One common process for the CPO and ATR cases (Fig. 6) and one for the SR case (Fig. 7). The CPO/ATR cycle consists of a blower (B301), heat preheater (E3), steam generator (E1), diesel pump, water pump, catalytic afterburner (CAT)

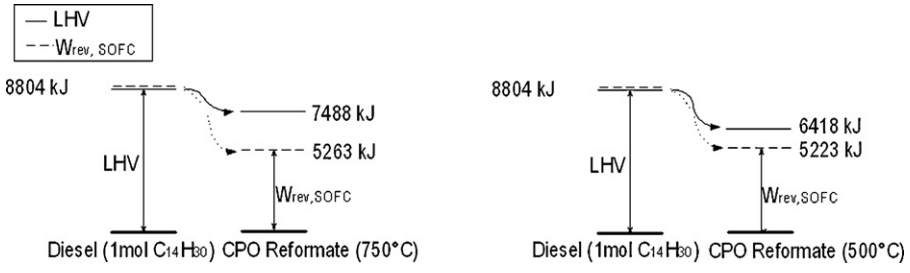

Fig. 3. Energy conversion of a catalytic partial oxidation at equilibrium ($C_{14}H_{30}$).

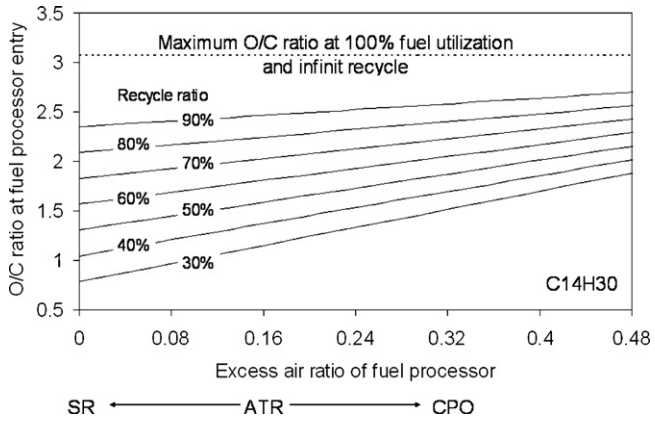

Fig. 4. Achievable O/C ratio for an anode recycle concept at fuel utilisation of 85% (total utilisation of residual fuel after CPO) vs. recycle ratio and excess air ratio of fuel processing ($C_{14}H_{30}$).

Table 3
Initial parameters of SOFC cycles.

Average cell voltage [V]	0.8
Fuel utilisation (SOFC single pass) [%]	70
Excess air fuel processor	0.6 (CPO); 0.47 (ATR); 0 (SR)
O/C ratio inlet fuel processor	2–2.5
Efficiency of blower (adiabatic) [%]	55
Pressure drop fuel processor [mbar]	20
Pressure drop E1, E3, CAT [mbar]	40
Pressure drop E7, E8 [mbar]	40
Thermal losses SOFC, HEX, combustor [%]	0
Parasitic power consumption [W]	50
Inverter efficiency [%]	96

and an inverter. No desulphurizer is considered for the CPO and ATR cases because the direct operation on ULSD with a sulphur level below 10 ppm wt. is feasible. Furthermore, it is assumed that the SOFC is able to handle around 1 ppm vol. sulphur in a long term operation perspective.

The steam reforming of diesel has been demonstrated with sulphur content around 1 ppm wt. A liquid desulphurisation is thus chosen to reduce the sulphur content of the ULSD from 10 ppm wt. down to 1 ppm wt. for the SR cycle (Fig. 7). The steam reforming requires heat particularly at operation temperatures of 750 °C or higher. The heat could be supplied by a catalytic afterburner which might be integrated in the steam reformer. At temperatures of around 500 °C an adiabatic operation is possible. In case of an adiabatic steam reforming, the system configuration would be similar to the CPO/ATR cycle (Table 3).

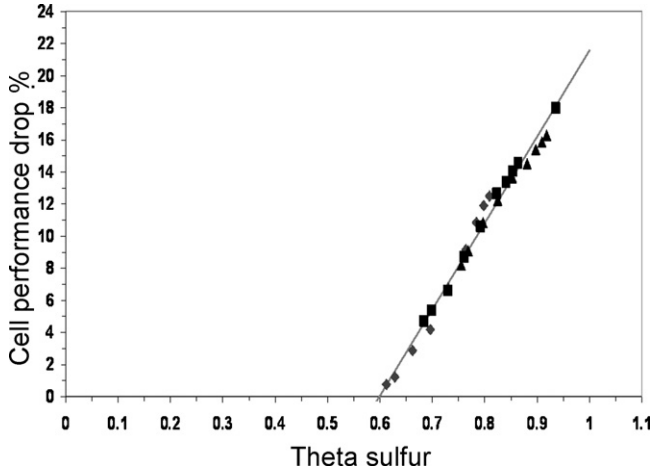

Fig. 5. Correlation of performance loss of Ni-YSZ cells vs. sulphur coverage by the correlation. Reproduced by permission of The Electrochemical Society, Copyright 2008.

All of the cycles are simulated for a fixed stack size with a constant number of cells, adjusting the fuel flow and the electrical current of the stack in order to maintain a constant average cell voltage of 0.8 V at a constant fuel utilisation of 70%. This fuel utilisation is a single pass fuel utilisation of the SOFC, which gives the electrochemical converted part of the fuel related to the maximum convertible at the anode entry. The SOFC's total fuel utilisation of the anode recycle concepts is higher than the single pass fuel utilisation. The total fuel utilisation is thus depending on the recycle ratio, which is governed by the required O/C ratio of the fuel processor (Fig. 4). The maximum convertible part of the fuel is defined to be the residual fuel after the CPO or ATR process. A total fuel utilisation of 100% is thereby achievable for all of the fuel processors.

The thermal balance of the adiabatic stack is simulated for fixed inlet anode and inlet cathode temperatures. The air flow is accordingly chosen to maintain a maximum cell temperature.

Fig. 8 illustrates the average coverage ratio of sulphur on the anode's nickel, simulated for the CPO, ATR and SR case (Table 4). Around 70% of the active sites of the nickel is covered by the sulphur for the steam reformer cycles and around 85% for CPO/ATR cycles. The coverage ratio is in this simulation independent from the recycle ratio because both, the sulphur and the hydrogen fraction change in a similar magnitude.

The ASR (Fig. 9) increases around 1% for the steam reformer and 9% for the CPO/ATR cases. The ASR is the average area specific resistance of the cell [$\Omega\,cm^2$] calculated by the average Nernst potential and average current density.

$$\mathrm{ASR} = \frac{\bar{E}_N - V_{cell}}{\bar{i}} \tag{13}$$

The power of the stack decreases in the same magnitude due to the fixed stack and the choice of a constant cell voltage for the design point. The activity of the internal reforming of methane in the SOFC changes inverse to the third power of the S/Ni coverage ratio [14,18]. The decrement in reforming activity is governed by a factor of 30 compared to the sulphur free reforming activity. The steam reforming case at 500 °C, resulting in methane content of around 15%, could not be simulated in a meaningful way because the reforming activity is too low in the anode.

The net power is strongly influenced by the required O/C ratio (Table 4). The net power decreases around 24–32% for the anode recycle cases by increasing the O/C ratio from 2 to 2.4. On the other hand the net efficiency increases around 2–4%-points caused by the higher total fuel utilisation. Slight increments in net efficiency are achieved by massive decrements in net power. The net efficiency of all of the cases could further be increased by optimising the system towards higher cell voltages, lower parasitic losses or using a larger stack but for illustration purposes this has been deliberately not chosen. The relative changes in net efficiency using different fuel processors would remain the same.

The trade-off between a more expensive system and a higher net efficiency has to be evaluated close to the requirements of the application. As long as there are no technical limits in increasing the O/C ratio from 2 to 2.5, there might be applications where higher O/C ratios and thus higher efficiencies will economically compensate the higher specific capital cost of the system (Fig. 10).

5. Economic comparison

The economic comparison is based on the equivalent annual cost (EAC). The EAC is the cost per year of owning and operating an asset over its entire lifespan. EAC is often used as a decision making

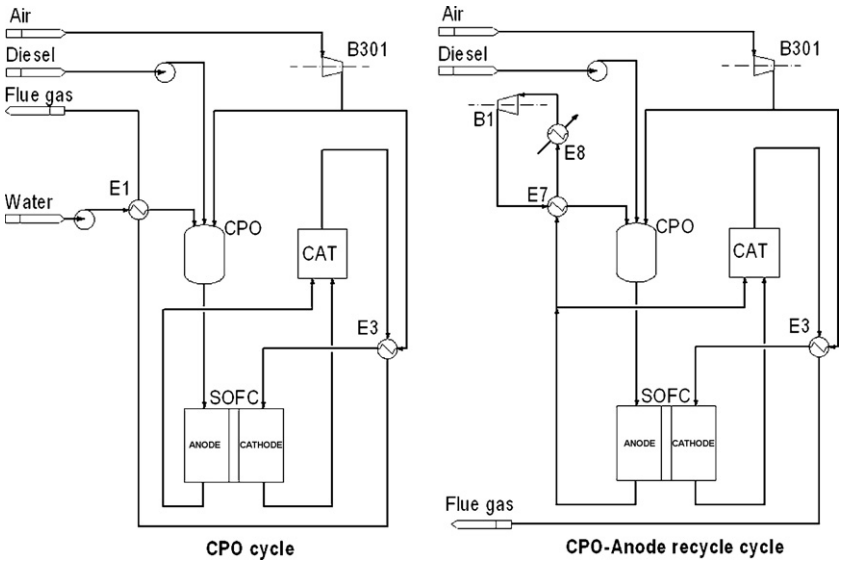

Fig. 6. CPO cycle (left: external water supply; right: with anode recycle).

Table 4
Simulation results.

Case		λ	S/C	O/C	η_{net} [%]	P_{net} [kW]
C0	CPO-external water	0.39	1.3	2.5	24.7	1.67
C1	CPO-anode recycle	0.39	0.452	2	29	1.6
C2	CPO-anode recycle	0.39	0.654	2.31	31.6	1.24
A0	ATR-external water	0.3	1.52	2.5	27.4	1.76
A1	ATR-anode recycle	0.3	0.525	2	34.1	1.58
A2	ATR-anode recycle	0.3	0.72	2.35	37.2	1.18
SL0	SR 530 °C-external water	0	2.5	2.5	–	–
SH0	SR 750 °C-external water	0	2.5	2.5	38	2.04
SH1	SR 750 °C-anode recycle	0	0.661	2	50	1.75
SH2	SR 750 °C-anode recycle	0	0.813	2.4	54	1.2

tool in capital budgeting when comparing investment projects. The EAC can be calculated by multiplying the net present value (NPV) of a project by the loan repayment factor LRF. The loan repayment factor (LRF) is calculated by the total time n (years) of the project and the discount rate i. The net present value (NPV) of a project or investment is defined as the sum of the present values of the annual cash flows C_i minus the initial investment C_0.

$$\mathrm{EAC_W} = \frac{1}{P_{\mathrm{net,average}} t_{\mathrm{annual}}} \left(C_0 \times \mathrm{LRF} \frac{P_{\mathrm{net,peak}}}{P_{\mathrm{net,average}}} + \frac{P_{\mathrm{net,average}} t_{\mathrm{annual}}}{\eta_{\mathrm{net}}} c_{\mathrm{fuel}} + C_{\mathrm{maintanace}} \right) \quad (14)$$

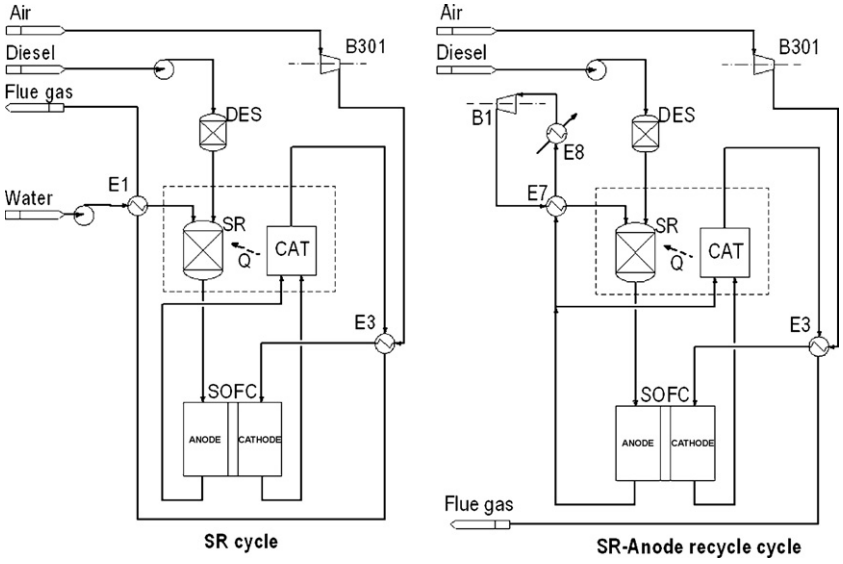

Fig. 7. Steam reformer cycles (left: external water supply; right: with anode recycle).

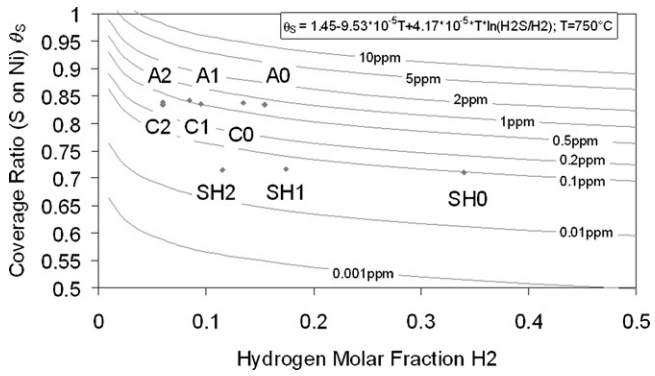

Fig. 8. Coverage ratio S on Ni vs. average hydrogen fraction at the anode (label description in Table 4).

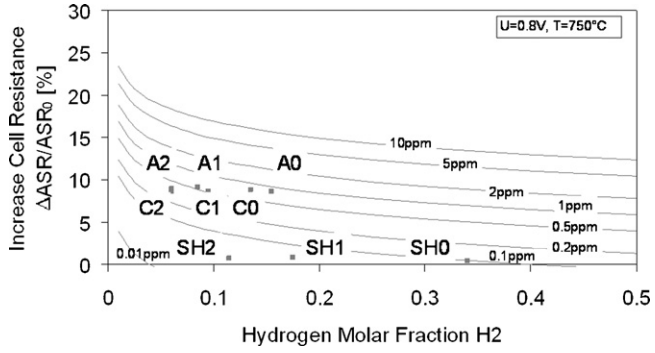

Fig. 9. Relative increment of ASR based on sulphur coverage on nickel vs. average hydrogen fraction at the anode (ASR expression reproduced from potentiostatic results for 0.8 V [11]; label description in Table 4).

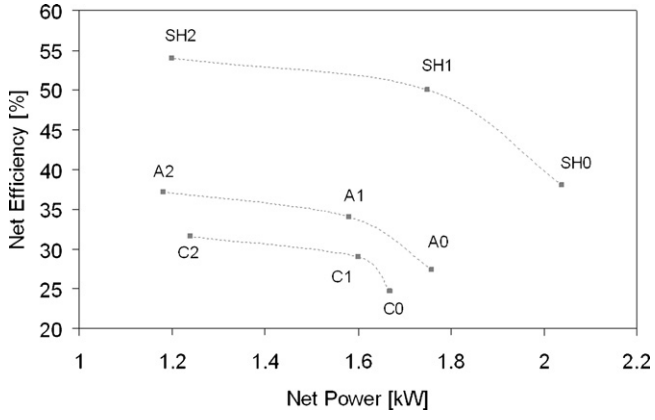

Fig. 10. Net power vs. net efficiency (label description in Table 4).

The specific EAC_W = 1.98$ kWh^{-1} of the truck idling application is calculated by the annual fuel and maintenance cost (thick full line; Fig. 11). Using the EAC_W of the truck idling application as maximum allowable cost for the SOFC APU would provide the break even capital cost of the SOFC APU for a known net efficiency and maintenance cost. Taking a certain payback time into account provides even lower allowable EAC_W for the SOFC APU. The maximum APU price can be calculated for different efficiencies in order to be able to estimate a slope which gives the allowable additional cost of the APU over a certain change in net efficiency.

As shown in Fig. 11, a fuel cell system with an average efficiency of 35% would be able to cost 2662$ kW^{-1} to ensure a payback time of 3 years. Around 90% of the fuel consumption during idling

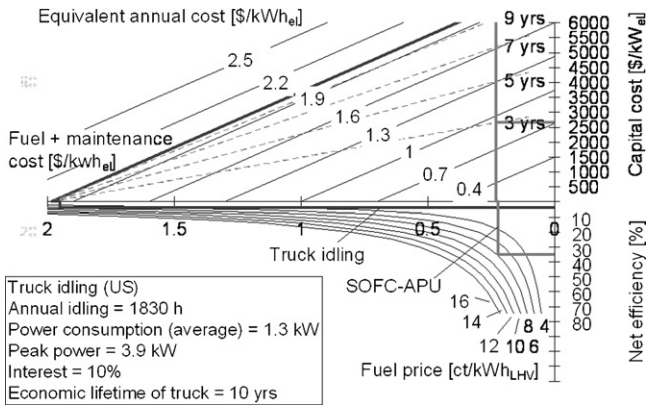

Fig. 11. Eco-map for the truck idling application.

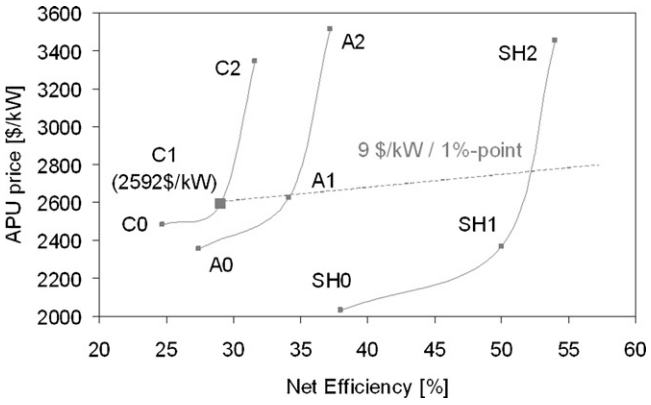

Fig. 12. APU price vs. net efficiency.

could be saved (Table 5). A higher efficiency allows higher capital cost for the same payback time. The APU price is allowed to increase from 2527$ kW^{-1} at 25% net efficiency to 2662$ kW^{-1} at 35% and 2738$ kW^{-1} at 45%. The additional APU price is 9$ kW^{-1} per percent point in efficiency increment for the range of 25–35% net efficiency. For higher efficiencies additional APU price is slightly lower.

The economic comparison of the fuel processing methods is simplified in the way that the capital cost of the system is not estimated by cost of the components. It is assumed that the allowable cost of SOFC-APU has already been achieved for the CPO case with an anode gas recycle (C1; 2592$ kW^{-1}). The price would be 10,100$ for a 3.9 kW SOFC-APU system. All of the system are based on the same stack size. The required air flow is equal comparing the CPO (C1), ATR (A1) and SR (SH1) case. The air preheater e.g. would have the same size for the different fuel processor cases. Thus, the ATR and SR systems are assumed to have the same total price as the CPO anode recycle case. This assumption overestimates the balance of plant (BOP) requirement towards higher O/C ratios whereas less net power and higher net efficiency requires less fuel and air flow to operate the system for the same stack size. The BOP components would be smaller than assumed. This overestimation will cost wise partly be compensated due to higher specific prices for smaller components.

Fig. 12 illustrates the specific APU prices which change exclusively with the net power for this comparison. The APU price of 10,100$ is fixed for the case C1 at a net power of 3.9 kW system. Starting from case C1 to A1 and comparing both cases with the allowable additional cost (dotted line; Fig. 12) shows that these both cases are economically equivalent. All cases which are above the doted line would require a longer payback-time than 3 years.

Table 5
Economic boundary conditions for truck idling (interest = 10%).

	Truck idling	SOFC-APU	SOFC-APU	SOFC-APU
Net efficiency	4%	25%	35%	45%
Power average [kWel]	1.3	1.3	1.3	1.3
Power peak [kWel]	3.9	3.9	3.9	3.9
Electrical work [kWh year^{-1}] (1830 h year^{-1})	2379	2379	2379	2379
Fuel consumption [gal year^{-1}] (37 kWh gal^{-1})	1607	257	183	142
Fuel cost [$ year^{-1}] (2.9$ gal^{-1})	4661	745	532	414
Maintenance cost [$ h^{-1}]	0.16	0.03	0.03	0.03
Maintenance cost [$ year^{-1}]	292	55	55	55
Variable cost (fuel + maintenance) [$ year^{-1}]	4953	800	587	469
Payback time [years]	–	3	3	3
Maximum APU price [$ kWel^{-1}]	–	2527	2662	2738
Δ max. APU price/Δ efficiency	–	9$ kW^{-1}/+1% to 7.6$ kW^{-1}/+1%		

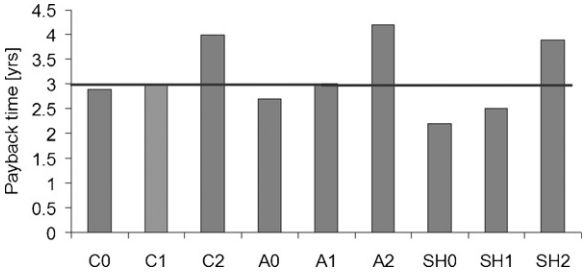

Fig. 13. Payback-time.

An increment in O/C ratio from 2 to 2.4 (case C1 to C2) for the CPO-recycle case e.g. causes a higher net efficiency of 2.6%-points and 22% less net power. The specific APU price would increase around 29%. The payback time would increase from 3 years to 4.1 years by increasing the O/C ratio from 2 to 2.4 (Fig. 13). Comparing the CPO case C1 and SH1 case will give a payback-time of 2.6 years instead of 3 years. There is a slight economic benefit in using an ATR or SR instead of a CPO for this application and under the assumption of equal APU prices. For this application it is economically very attractive to be able to operate the fuel processors at the lowest O/C ratio as possible.

6. Conclusion

It is concluded that a diesel based SOFC APU system is an attractive option even with the present fuel prices given a realistic cost for the system. The electrical net efficiency of the simulated SOFC-APUs implying CPO, ATR and SR fuel processors vary in broad range between 25% and 54%. Around 32% of the diesel is pre-combusted within the CPO. An equivalent amount of electrons which could contribute to the work, generated in the downstream SOFC, is lost by the partial oxidation. The loss of reversible work, which could be potentially converted in the SOFC to electrical work, is around 41.5%. The total exergetic efficiency (86–89%) is much higher than the intrinsic exergetic efficiency (58.5%). Low O/C ratio operation is very beneficial for CPO operation. A decrement of the O/C ratio from 2.4 to 2 reduces the payback time around 25%. A rough economic estimate shows that the ATR and SR is slightly better than the CPO for this specific application. It seems feasible to operate the SOFC APU without a desulphurisation unit if ULSD quality is used as the penalty even using traditional Ni-YSZ anodes is relatively modest.

References

[1] http://www.polk.com/KC/PolkAR-CVR-200912.pdf.
[2] http://epa.gov/smartway/presentations/background.pdf.
[3] http://www.arb.ca.gov/fuels/diesel/dieselcomp/010809prsntn.pdf.
[4] F. Stodolsky, L. Gaines, A. Vyas, Argonne National Laboratory, ANL/ESD-43, 2000.
[5] C.I. Sishtla, K. Krist, D.A. Suchorabski, J.M. Pondo, Fuel Cell Seminar, Palm Springs, CA, Poster 78, 2005.
[6] W. Winkler, P. Nehter, M.C. Williams, Resources Processing 56 (1) (2009) 8–12.
[7] T.S. Christensen, Applied Catalysis A: General 138 (1996) 285–309.
[8] J. Pasel, J. Latz, Z. Pors, J. Meißner, R.C. Samsun, A. Tschauer, ECS Transaction 12 (1) (2008) 589–600.
[9] T. Aicher, B. Lenz, F. Gschnell, U. Groos, F. Federici, L. Caprile, L. Parodi, Journal of Power Sources 154 (2006) 503–508.
[10] J.B. Hansen, J. Rostrup-Nielsen, Handbook of Fuel Cells, vol. 6, John Wiley and Sons Ltd, 2009 (Chapter 65).
[11] J.P. Trembly, A.I. Marquez,.T.R. Ohrn, D.J. Bayless, Journal of Power Sources 158 (2006) 263–273.
[12] O.A. Marina, L.R. Pederson, C.A. Coyle, E.C. Thomsen, G.W. Coffey, ECS Transaction 25 (2) (2009) 2125–2130.
[13] J.B. Hansen, Electrochemical and Solid State Letters 11 (10) (2008) B178.
[14] F. Silversand, J.B. Hansen, A.K. Jannasch, J. Pålsson, Fuel Cell Seminar, Honolulu, HI, Poster 111, 2006.
[15] K. Sasaki, K. Susuki, A. Iyoshi, M. Uchimura, N. Imamura, H. Kusaba, Y. Teraoka, H.H. Fuchino, K. Tsujimoto, Y. Uchida, N. Jingo, Proceedings: Electrochemical Society PV 2005–2007 (2005) 1267–1274.
[16] J.N. Kuhn, N. Lakshminarayanan, U.S. Ozkan, Journal of Molecular Catalysis A: Chemical 282 (1–2) (2008) 9–21.
[17] H.P. He, A. Wood, D. Steedman, M. Tilleman, Solid State Ionics 179 (27–32) (2008) 1478–1482.
[18] J.R. Rostrup-Nielsen, Journal of Catalysis 85 (1984) 31.